JOURNAL OF CATALYSIS **169,** 228–239 (1997)
ARTICLE NO. CA971663

Ab Initio MO-LCAO Investigation of the Structure and Reactivity towards Alkenes of Model Tungsten(VI) Peroxo Complexes Derived from the Tetrakis (Oxodiperoxotungsto) Phosphate(3-) Complex, $\{PO_4[W(O)(O_2)_2]_4\}^{3-}$

P. Fantucci,*,[1] S. Lolli,* and C. Venturello†

*Department of Inorganic, Metallorganic and Analytical Chemistry, CNR Center, University of Milan, Via Venezian 21, 20133 Milan, Italy; †Istituto G. Donegani SpA EniChem Ricerche, Via G. Fauser 4, 28100 Novara, Italy

Received July 31, 1996; revised October 10, 1996; accepted January 28, 1997

An *ab initio* MO-LCAO investigation was undertaken concerning the structure and reactivity towards alkenes of model tungsten(VI) peroxo complexes derived from the tetrakis (oxodiperoxotungsto) phosphate(3-) complex, $\{PO_4[W(O)(O_2)_2]_4\}^{3-}$, an efficient reagent (as "onium" salt) for olefin epoxidation in nonprotic solvents, as well as a highly effective catalyst for the same reaction when used in combination with hydrogen peroxide in a two-phase system. The complex of formula $[H_2PO_4(W_2O_{10})]^-$ (A), chosen as a simplified model of the $\{PO_4[W(O)(O_2)_2]_4\}^{3-}$ anion, and the related "partially reduced" complexes of general formula $[H_2PO_4(W_2O_9)]^-$ ($B_{1,2}$) and $[H_2PO_4(W_2O_8)]^-$ (C_{1-3}) were considered. The best molecular geometries for all the investigated complexes were obtained at Hartree–Fock level, using a relativistic effective potential for core electrons of the W atoms. The Hartree–Fock energies corrected for electron correlation by means of Lee–Yang–Parr density functional were used to evaluate the reaction energies regarding the peroxidic oxygen transfer from complexes A and $B_{1,2}$ to an alkene (ethylene). The energetics of these complexes is discussed in the framework of a global process leading to the formation of epoxide and restoring the starting complexes by reaction of the resulting "reduced" species with hydrogen peroxide. All the reaction steps, identified on the basis of a purely theoretical investigation, were found to be, to a different extent, exothermic. The analysis of the net atomic charges carried by the peroxidic oxygens in complexes A and $B_{1,2}$ reveals that the oxygen expected to be the "most electrophilic" is the one adjacent to the triply shared oxygen. Its transfer to ethylene is associated with the highest energy gain when complex A is involved, but such a behaviour is no longer regularly observed when a complex of type B is considered.

1. INTRODUCTION

The metal-catalysed epoxidation of olefins by aqueous hydrogen peroxide has received considerable attention in recent years (1) in view of the fact that this oxidant is cheap, safe, and environmentally clean. The search for suitable metal catalysts has centred mainly around high valent group 5a,b and 6a,b metal oxides, which are known (1b, 2) to react with hydrogen peroxide to form "end-on" or "side-on" metal peroxide species capable of readily oxidising olefinic double bonds via an electrophilic oxygen transfer.

In this context, some years ago, we found the association of tungstate and phosphate (or arsenate) ions under acidic conditions to be an efficient catalytic system for olefin epoxidation by hydrogen peroxide according to the phase-transfer technique (3). The $\{XO_4[W(O)(O_2)_2]_4\}^{3-}$ anionic side-bonded peroxotungsten species **1** (X = P or As), in association with a lipophilic, long chain quaternary cation (Q^+), was proposed as the active oxidant. Indeed, the isolated "onium" salts of **1**, namely quaternary ammonium (phosphonium) tetrakis(oxodiperoxotungsto)phosphates or -arsenates(3-), $Q_3XO_4[W(O)(O_2)_2]_4$ (Q-**1**), proved to be good reagents for the epoxidation of simple, inactivated alkenes in nonprotic solvents, as well as highly effective catalysts for the same reaction when employed in conjunction with hydrogen peroxide as the terminal oxidant in an aqueous/organic biphase system (4). By using various Q-**1** salts (X = P) as catalysts, especially those with $Q^+ = [(C_8H_{17})_3 \cdot NCH_3]^+$ or $\{[C_{18}H_{37}(75\%) + C_{16}H_{33}(25\%)]_2N(CH_3)_2\}^+$, a versatile and synthetically valuable methodology for the epoxidation of water insoluble alkenes with even very dilute (15%) hydrogen peroxide was developed (5), which has already been successfully applied to the production of epoxides of commercial interest and, also, to the epoxidation of unsaturated polymers (6), a well-studied and important reaction.

Aside from the synthetic aspect, the high epoxidizing ability of **1** attracted our interest from the speculative point of view. Indeed, anionic d^0 early-transition-metal peroxo complexes are known to be poor to modest electrophilic oxidants (7). The reason why, by contrast, the anionic peroxo

[1] Correspondence to: Piercarlo Fantucci, Department of Inorganic, Metallorganic and Analytical Chemistry, University of Milan, Via Venezian 21, 20133 Milan, Italy. Phone-fax: 0039-2-26680678; E-mail: fant@inorg141.csmtbo.mi.cnr.it.

0021-9517/97 $25.00

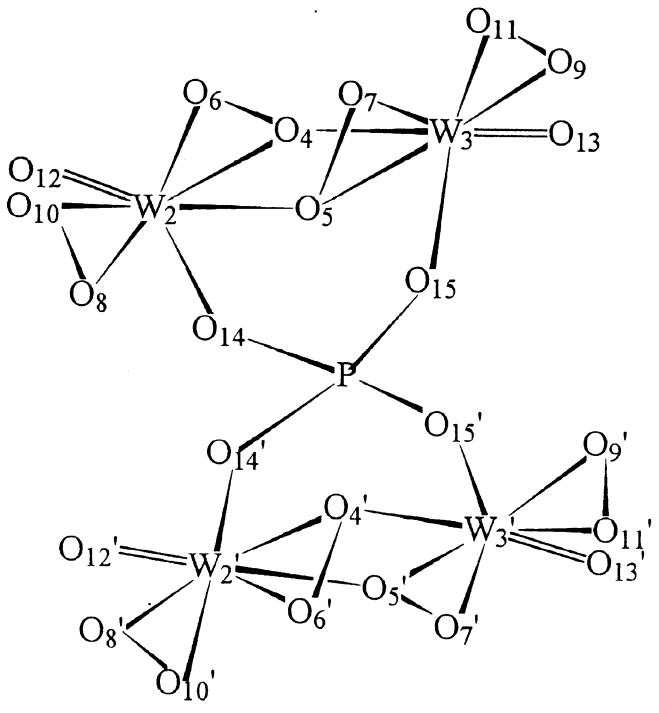

FIG. 1. View of the $\{PO_4[W(O)(O_2)_2]_4\}^{3-}$ anion in THX-**1** (X = P) (4).

species **1** can transfer oxygen readily to weak nucleophiles such as alkenes still remains rather unclear. It was suggested (4) that this might depend on an enhanced electrophilic character of the peroxo moieties due to the unusual presence of triply shared peroxo oxygens, as revealed by the crystal structure of the tetrahexylammonium salt of **1**, THA-**1** (X = P) (4), which shows the anion to consist of four distorted $W(O)_3(O_2)_2$ pentagonal bypiramids in edge-shared pairs, each sharing oxygen with a central tetrahedral PO_4 group (Fig. 1). In fact the presence of a double bridge, where each of the two shared bridge oxygens in turn participates to a side-bonded peroxo moiety, makes one of the two bidentate peroxo ligands coordinated to the metal markedly dissymmetric. More recently, the view was advanced (8) that a varying degree of dissymmetry of the O–O bonds, which would increase the electrophilic character of one of the peroxo oxygen atoms at the expense of the other, thereby facilitating nucleophilic attack by the alkene on the peroxide, might be responsible in general for the different reactivities of the oxodiperoxometalates and their heteropoly derivatives toward olefinic substrates.

In an attempt to shed some light on this point, we undertook a theoretical study aimed at testing the proneness of the various peroxidic oxygens of **1** (X = P) to be transferred to alkene. As can be noted from inspection of Fig. 1, in the $\{PO_4[W(O)(O_2)_2]_4\}^{3-}$ anion each of the two dimeric $[W(O)(O_2)_2]_2$ units (held together by the central phosphate group) contains three types of structurally nonequivalent peroxidic oxygen atoms, one of them concerning the oxygens of the nonbridging (or normal) peroxo groups, the other two concerning the oxygens of the bridging peroxo groups. It seems therefore reasonable to expect these different types of oxygen to exhibit also a different electrophilic character.

Rigorously, the evaluation of their aptitude to interact with an alkene would require the computation of the activation energy pertaining to their transfer from the $\{PO_4[W(O)(O_2)_2]_4\}^{3-}$ anion to the olefinic substrate. However, owing to the dimension of the system under study, such an approach appeared too burdensome from a computational point of view. We therefore deemed it more convenient for a preliminary theoretical study to limit our investigation to evaluating the thermodynamic aspects of the above oxygen transfer reactions, in the hypothesis that, in the present case, the differences in transition state energies do not markedly change the trend of the final states. This implied the problem of determining (with *ab initio* calculations) the geometric and electronic structures of the metal species involved in these oxygen transfer reactions from the $\{PO_4[W(O)(O_2)_2]_4\}^{3-}$ anion to alkene, which also included the ones concerning the transfer of a second peroxidic oxygen to the olefinic substrate.

On the basis of the values of the net charges computed for each of the potentially transferable peroxidic oxygens of the metal species taken into account, we were then interested in establishing whether the oxygen expected to be the "most electrophilic" was also the one associated with the highest energy gain in the epoxidation reaction. The results of this study are here reported.

2. COMPUTATIONAL METHOD

The theoretical investigation was carried out in the framework of the *ab initio* Hartree–Fock (HF) method, using a relativistic effective core potential (ECP) operator to represent the $(1s^2 2s^2 \cdots 4d^{10} 4f^{14})$ core of the W atom (9) considered as a 14-valence electron atom. The valence space is spanned by 5*s*, 5*p*, 5*d*, 6*s*, and 6*p* atomic orbitals (AO) which are described by a Gaussian basis of type (311/32/21) (9). A split-valence basis STO 3-21G (10) was adopted for the hydrogen, carbon, oxygen, and phosphorus atoms. Preliminary calculations on the phosphate group showed that a *d* polarisation function ($\xi = 0.5$) on the P atom is necessary in order to obtain a reasonable description of the P–O bond length. The same polarisation function was adopted for the P atom in the tungsten complexes examined.

In order to avoid biased energy results due to the assumed molecular structures of the various chemical species involved in this study, all the tungsten complexes and the other molecules considered, i.e., ethylene, ethylene oxide, hydrogen peroxide, and water, were subjected to a full HF

geometry optimisation (11). In general, the structures of the tungsten complexes were obtained without imposing symmetry constraints, with the exception of complex **A**, $\{(H_2PO_4[W(O)(O_2)_2]_2\}^-$ (see next section), which is supposed to posses a C_2 symmetry. Such an idealised symmetry is not present in the X-ray structure of **1** (X = P) (4), but it can be postulated in the gas phase due to the equivalence of the coordination spheres of the two W atoms. The constraint-free geometry optimisation avoids the fact that the procedure can lead to saddle points, but does not necessarily give a global minimum. On the other hand, the existence of several isomers low lying in energy can be considered as unprobable because each metal centre tends to realise in a quite rigid manner the highest possible coordination number (see Section 2).

In order to improve the energy values given by the HF approach, the interelectron correlation energy was added. It was obtained by means of the Lee, Yang, and Parr (LYP) density functional (12) as post-HF corrections computed in the HF minimum geometry using the HF converged density (see also Refs. (13) and (14) for computational details and applications).

The electron distribution was computed according to the Mulliken's partition scheme (15). Owing to the arbitrariness of such a procedure (16) (and of other related procedures), orbital occupancies and gross atomic charges were used only for a qualitative discussion of the electronic structure/reactivity relationship for the various peroxidic oxygens of the examined tungsten complexes (see Section 4), while a more grounded discussion of the reactivity of the latter was based on the energy values computed according to the correlated HF-LYP scheme (E_{LYP}) (see Section 3).

3. RESULTS AND DISCUSSION

3.1. Choice of a Model Peroxo Complex

In order to pursue our aim, we first focused on the computation of the electronic and geometrical structure of the $\{PO_4[W(O)(O_2)_2]_4\}^{3-}$ complex. However, the size of the latter proved too large for a systematic *ab initio* MO-LCAO investigation (at the present level of accuracy, the basis set would include more than 250 functions). We therefore decided to consider, as the starting species for our study, a simplified complex, $\{H_2PO_4[W(O)(O_2)_2]_2\}^-$ (here denoted as **A**), which contains just half the original anion, with two valencies of the phosphate group saturated by hydrogen atoms. The geometrical and electronic structure of this model complex was determined by quantum-chemical calculations. The computed molecular structure is shown in Fig. 2.

As can be seen from the comparison of Figs. 1 and 2, the theoretical molecular structure found for complex **A** satisfactorily agrees with the structural features of the original $\{PO_4[W(O)(O_2)_2]_4\}^{3-}$ anion. Recently, an anionic tungsten

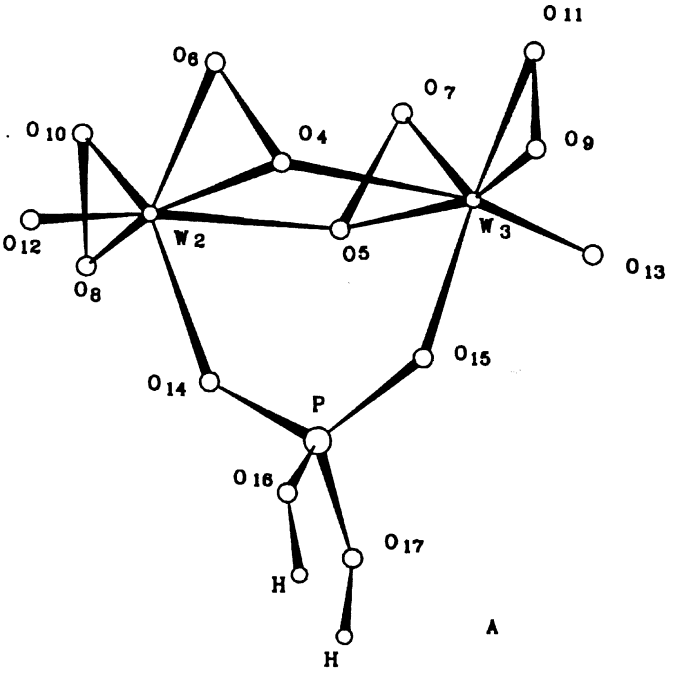

FIG. 2. Theoretically optimized structure of the model complex **A** of formula $[H_2PO_4(W_2O_{10})]^-$.

species very closely related to complex **A**, having just one acidic hydrogen, $\{HPO_4[W(O)(O_2)_2]_2\}^{2-}$, has actually been isolated as the $[n\text{-}Bu_4\mathbf{N}]^+$ salt and characterised by X-ray diffraction analysis (Fig. 3), as well as by ^{31}P and ^{183}W NMR spectroscopy (17). This novel complex, hereafter referred to as **A'**, has been shown to be an active oxygen-to-olefin transfer agent (17).

The main features of the geometric structure of complex **A** will be now discussed in detail.

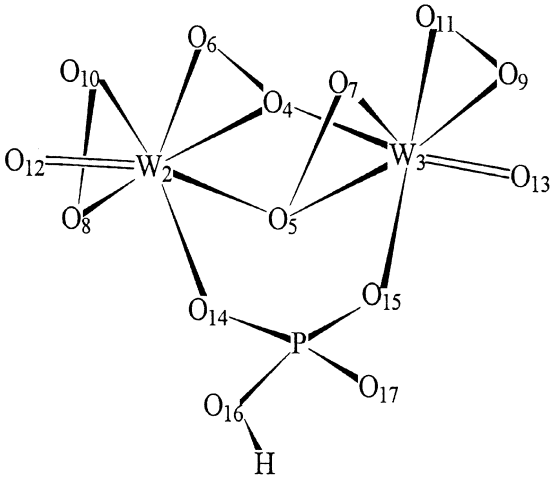

FIG. 3. View of the $\{HPO_4[W(O)(O_2)_2]_4\}^{2-}$ anion in the tetrabutylammonium salt (17).

3.2. The $[H_2PO_4(W_2O_{10})]^-$ Complex (**A**)

HF-ECP geometry optimisations have been carried out on model complex **A** and its analog **A'**. The most relevant structural parameters are reported in Table 1 and compared with the experimental data of the complex **1** (X = P) (4) and **A'** (17). Such a comparison, however, needs special care, due to the fact that in the solid state the coordination spheres of the two W atoms in each $[W(O)(O_2)_2]_2$ unit are not exactly symmetry related. The comparison between theory and experiment will be based on mean values.

As for the W–O bonds, the theory predicts distances which are probably too long, in average, by about 0.05–0.08 Å. However, also, the experimental data of the two complexes $[PO_4(W_4O_{20})]^{3-}$ (4) and $[HPO_4(W_2O_{10})]^{2-}$ (17) concerning the W–O bond lengths differ by even more than 0.1 Å. As for the valence angles W–O–W and O–W–O our computed values are within (or at the border of) the range of the experimental data.

We can conclude that, despite the fact that our geometry optimisation was carried out neglecting the interelectron correlation, the general agreement between theoretical and experimental data for both complexes **A** and **A'** indicates that our computational approach can give a reliable estimate of the coordination geometries. In particular, also, the rather unusual coordination of the tungsten atoms, involving both normal and bridging peroxo groups and leading to the formation of asymmetric dimeric units $[W(O)(O_2)_2]_2$ in which the two associated pentagonal bypiramides share one edge of the nonbasal plane, may be predicted in a substantially correct manner. The presence of this dimeric unit, which appears to be a peculiar feature of the $[PO_4(W_4O_{20})]^{3-}$ and $[HPO_4(W_2O_{10})]^{2-}$ anions, is confirmed also by our calculations in a noncondensed phase as an essential constituent of the stability of these complexes.

As commented above, the correlation effects, here neglected, are expected to induce only marginal modifications in the geometries which cannot substantially modify the computed stability of complex **A** and of the related "partially reduced" complexes (see below) as well as their reaction energies.

These results, while pointing to the validity of the present computational method, ensure the reliability of the model complex chosen for the planned work.

3.3. The "Partially Reduced" Metal Species (Related to Complex **A**) Considered in the Oxygen Transfer to Alkene

We then passed to calculate the structures of the metal species related to peroxo complex **A** (here considered as the basic species) that originate from it by successive removal of one or two peroxidic oxygens. The theoretically

TABLE 1

Theoretically Evaluated Geometrical Parameters for the Model Complex A $[H_2PO_4(W_2O_{10})]^-$ and its Analog, $[HPO_4(W_2O_{10})]^{2-}$ (A'), Compared with the Experimental Ones

Geometrical parameter[a]	Computed value for		Experimental values for	
	$[H_2PO_4(W_2O_{10})]^-$ [b]	$[HPO_4(W_2O_{10})]^{2-}$ [c]	$[PO_4(W_4O_{20})]^{3-}$ [d]	$[HPO_4(W_2O_{10})]^{2-}$ [e]
W_2O_4–W_3O_5	2.01	2.03	1.95–2.03	1.92–1.94
W_2O_5–W_3O_4	2.42	2.36	2.41–2.51	2.34–2.34
W_2O_6–W_3O_7	1.94	1.95	1.85–1.92	1.86–1.93
W_2O_{10}–W_3O_{11}	1.93	1.94	1.84–1.88	1.90–1.89[f]
W_2O_8–W_3O_9	1.93	1.95	1.88–1.97	1.97–1.92
O_8O_{10}–O_9O_{11}	1.51	1.51	1.63–1.51	1.53–1.56
W_2O_{12}–W_3O_{13}	1.69	1.70	1.65–1.62[g]	1.62–1.71
W_2O_{14}–W_3O_{15}	2.06	1.97	1.96–1.96	1.92–1.94
O_4O_6–O_5O_7	1.50	1.50	1.43–1.56	1.51–1.47
PO_{14}–PO_{15}	1.54	1.56	1.58–1.53	1.58–1.55
PO_{16}–PO_{17}	1.58	1.61, 1.47[h]	1.53–1.58	1.52–1.48
$W_2O_5W_3$–$W_2O_4W_3$	112.1	110.3	106.8–105.6[g]	111.2–110.8
$O_4W_2O_5$–$O_4W_3O_5$	67.5	68.8	74.8–71.2[g]	68.6–68.3

[a] See Figs. 1, 2, and 3 for the atomic numbering scheme. Bond distances, Å; valence angles, degrees.

[b] A single value is given for each pair of parameters since complex **A** is assumed to possess a $\mathbf{C_2}$ symmetry, lacking in the X-ray structure of the $[PW_4O_{24}]^{3-}$ and $[HPW_2O_{14}]^{2-}$ complexes (see Computational method).

[c] Average values for pair for internal coordinates.

[d] From the X-ray diffraction analysis of THX-**1** (X = P) (4).

[e] From the X-ray diffraction analysis of $(n\text{-}Bu_4N)_2[HPW_2O_{14}]$ (17).

[f] Reference (17) reports the value 1.66 Å, which is unacceptably low for this kind of bond. The figure 1.89 Å has been recomputed by assuming that the *x*/*a* value for O(10) in Table 2 of Ref. (17) should have changed sign.

[g] Values derived from the geometry relationship.

[h] Distance between phosphorous and unprotonated oxygen atom.

determined molecular structures of these "partially reduced" species, which are here denoted as $\mathbf{B_{1,2}}$ (with general formula $[H_2PO_4(W_2O_9)]^-$) and $\mathbf{C_{1-3}}$ (with general formula $[H_2PO_4(W_2O_8)]^-$), are shown in Figs. 4 and 5, respectively.

For the sake of clarity, the four types of structurally nonequivalent oxygen atoms present in the dimeric $[W(O)(O_2)_2]_2$ unit of complex **A** (three of which, as shown before for the original complex **1** (X = P), concerning the peroxidic oxygens) will be labelled henceforth as O_s, O_d, O_{t1}, and O_{t2}, respectively. O_s indicates oxo oxygen atoms (W=O) (O_{12} and O_{13} atoms of Fig. 2). O_d indicates the oxygen atoms of the nonbridging (or normal) peroxo groups (O_8, O_9, O_{10}, and O_{11} atoms of Fig. 2). Finally, O_t indicates the oxygen atoms of the bridging peroxo groups; in particular O_{t1} indicates the oxygen atom bound to a single tungsten atom (O_6 and O_7 atoms of Fig. 2) while O_{t2} indicates the triply shared oxygen atom, which also forms a long W–O bond with a second tungsten centre (O_4 and O_5 atoms of Fig. 2). Unlike the oxygen atoms of the bridging peroxo groups, the two oxygens of the normal peroxo groups are not differentiated in our labelling scheme, as they are expected to be chemically nearly equivalent. The close similarity of the two O_d oxygens is confirmed also by the analysis of their Mulliken electron population (see Section 4).

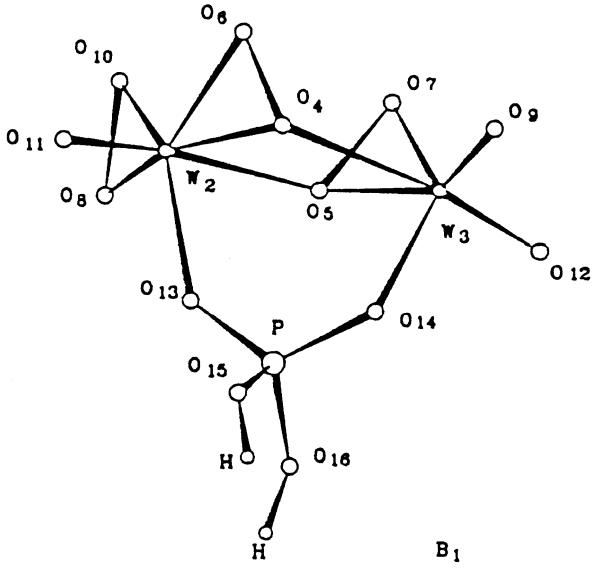

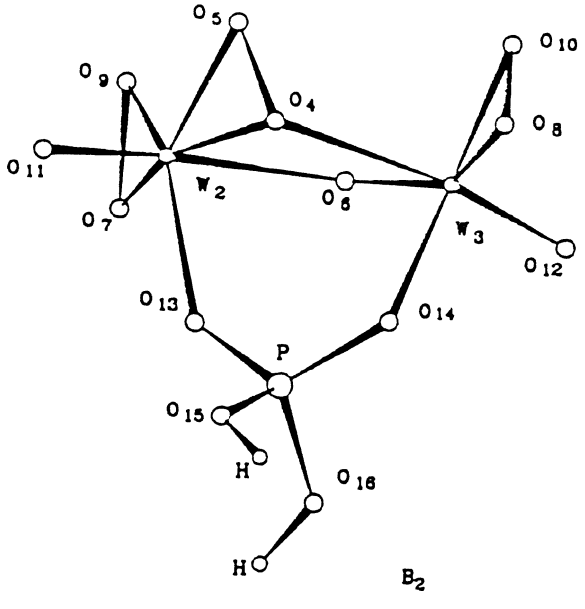

FIG. 4. Theoretically optimized structures of the complexes $\mathbf{B_{1,2}}$ of general formula $[H_2PO_4(W_2O_9)]^-$.

Following the above labelling scheme, the isomeric species $\mathbf{B_1}$ and $\mathbf{B_2}$, shown in Fig. 4, are generated from species **A**, according to the general equation [1], when one peroxidic oxygen of type O_d (belonging to a normal O_2 group) and of type O_t (belonging to a bridging O_2 group), respectively, is supposed to be transferred to an olefinic substrate, which is here assumed to be the simple ethylene molecule,

$$A + C_2H_4 \rightarrow B_x + C_2H_4O \quad (x = 1, 2). \qquad [1]$$

It should be noted that the removal of one oxygen of type O_{t1}, rather than of type O_{t2}, from **A** is equivalent from the computational point of view, since it leads univocally to the same species $\mathbf{B_2}$, which ensures the highest coordination number for each tungsten atom.

Analogously, the isomeric species $\mathbf{C_1}$, $\mathbf{C_2}$, and $\mathbf{C_3}$, shown in Fig. 5, are generated from the intermediate species $\mathbf{B_1}$ and $\mathbf{B_2}$, according to the general equation [2], when a second peroxidic oxygen (again of type O_d, or type O_t) is supposed to be transferred to ethylene, to give an additional molecule of epoxide,

$$B_x + C_2H_4 \rightarrow C_y + C_2H_4O \quad (x = 1, 2;\ y = 1\text{–}3). \qquad [2]$$

In considering the complexes of type **C**, the species obtainable on reduction of the oxomonoperoxotungsten moieties of $\mathbf{B_1}$ and $\mathbf{B_2}$ were neglected, since the release of peroxidic oxygen from such units to alkene is known to occur with much more difficulty (7a, 18), as confirmed, on the other hand, by the behaviour of the $\{PO_4[W(O)(O_2)_2]_4\}^{3-}$ (4, 19) and $\{HPO_4[W(O)(O_2)_2]_2\}^{2-}$ (17) complexes, for which nearly half the peroxidic oxygen available can be transferred to alkene.

All the species considered in this study that originate from complex **A** by successive removal of one or two

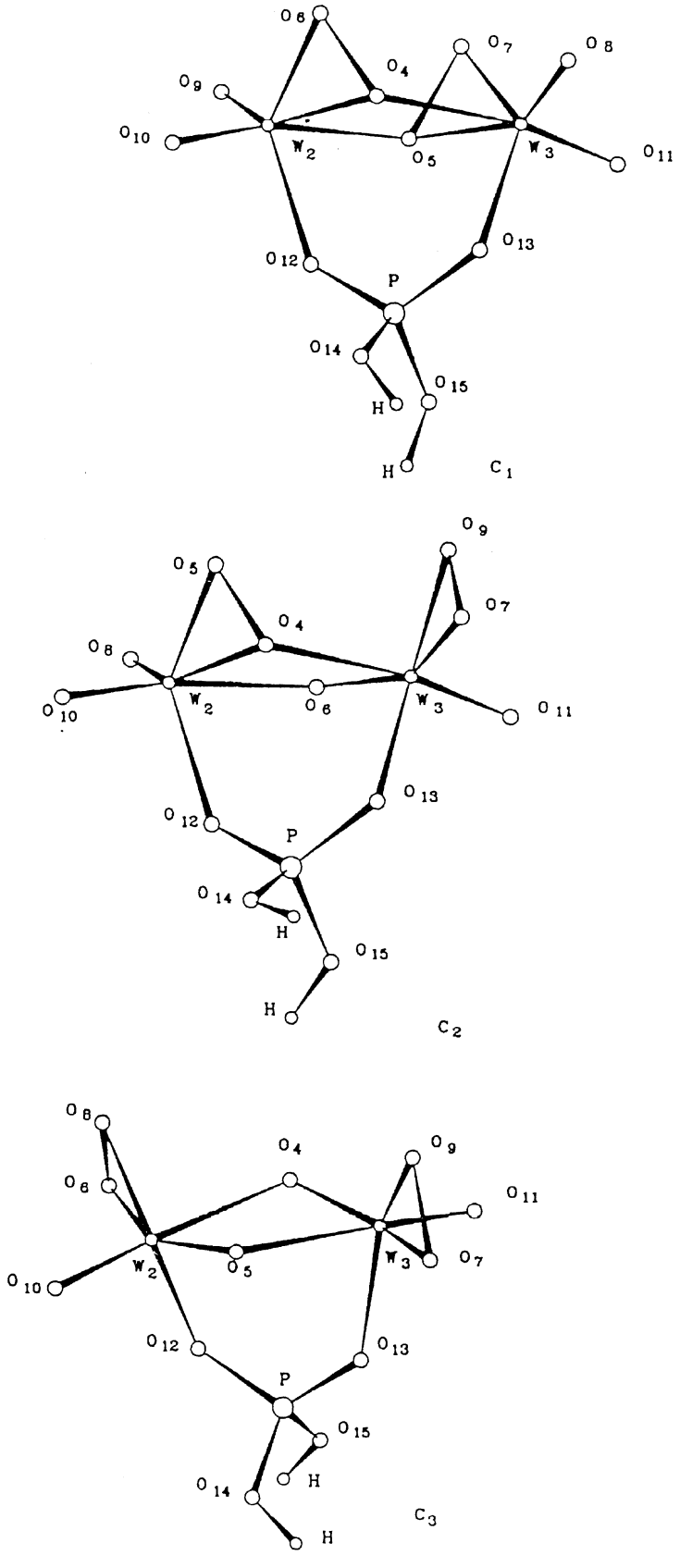

FIG. 5. Theoretically optimized structures of the complexes $\mathbf{C_{1-3}}$ of general formula $[H_2PO_4(W_2O_8)]^-$.

peroxidic oxygen atoms of type O_d and/or O_t are summarised in a schematic way in the chart.

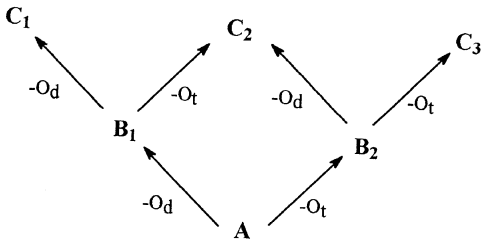

The general agreement found between the theoretical molecular structure of the model complex **A** and the experimental molecular structures of the $\{PO_4[W(O)(O_2)_2]_4\}^{3-}$ and $\{HPO_4[W(O)(O_2)_2]_2\}^{2-}$ complexes allows us to assume that also the geometry (and stability) of the complexes of type **B** and **C**, for which no experimental data are available for comparison, can be theoretically evaluated at a reasonable level of confidence.

The main features of the geometric structure of complexes $\mathbf{B_{1,2}}$ and $\mathbf{C_{1-3}}$ will be now discussed in detail.

*The $[H_2PO_4(W_2O_9)]$ complexes (**B**).* In isomer $\mathbf{B_1}$, one of the two W atoms (indicated as W_3 in Fig. 4) is directly bound to two terminal O_s atoms and becomes hexacoordinated. The two W(3)-O_s bond distances are nearly identical (1.71 Å) but considerably longer than the W(2)-O_s bond distance (1.69 Å) (see Table 2). The O–O distances for the two bridging peroxo groups (O_4O_6, O_5O_7) now bound to nonequivalent metal centres, become nearly identical (1.51 Å). The W(2) and W(3) metal atoms are both involved in long- and short-distance bonds with O_{t2} oxygen atoms. The extent to which complex $\mathbf{B_1}$ has lost symmetry with respect to its precursor **A** is clearly shown by the differences existing between the two long and the two short W-O_{t2} bond distances. For W(2) the computed values were 2.29 and 2.01 Å, and for W(3), 2.41 and 2.07 Å, respectively (see Table 2). This indicates that the hexacoordination which W(3) has been forced to assume makes its interaction with the bridging O_2 group weaker. On the contrary, W(2) keeps its heptacoordination and an overall coordination geometry fairly close to that found in complex **A**, with the exception of the W(2)-O(5) bond which is characterised by a distance shorter than that found in complex **A** (2.29 vs 2.42 Å).

The structure of isomer $\mathbf{B_2}$, which was obtained without any symmetry constraint, includes an oxygen atom bridging two W atoms with one short and one long W–O bond distance. As for the spatial location, such an oxygen atom is similar to the O_{t2} atoms in complex **A** and its presence is necessary to preserve the heptacoordination, at least for one of the two W centres. As reported in Table 2, the bond distances for $\mathbf{B_2}$ are equal to those computed for isomer $\mathbf{B_1}$ within about ±0.03 Å.

On the basis of the E_{LYP} energies (Table 3), complex $\mathbf{B_2}$ becomes 15.6 kJ · mol^{-1} more stable than isomer $\mathbf{B_1}$.

*The $[H_2PO_4(W_2O_8)]$ complexes (**C**).* In Fig. 5 the molecular structures of the three isomers of type C are schematically shown and are all characterised by two hexacoordinated W atoms. The hexacoordination is ensured by the presence of two bridging O_2 groups in $\mathbf{C_1}$, one bridging the O_2 and one bridging the oxygen atom in $\mathbf{C_2}$ and two

TABLE 2

Theoretically Evaluated Geometrical Parameters for Complexes $[H_2PO_4(W_2O_9)]^-$ (B)

Geometrical parameter[a]	$\mathbf{B_1}$ computed value	Geometrical parameter[a]	$\mathbf{B_2}$ computed value
W_2O_4–W_3O_5	2.01–2.07	W_2O_4–W_3O_6	2.03–1.79
W_2O_5–W_3O_4	2.29–2.41	W_2O_6–W_3O_4	2.22–2.39
W_2O_{10}–W_2O_8	1.92–1.94	W_2O_9–W_2O_7	1.92–1.94
W_2O_6–W_3O_7	1.95–1.94	W_3O_{10}–W_3O_8	1.90–1.95
W_2O_{11}	1.69	W_2O_{11}–W_3O_{12}	1.70–1.70
W_3O_9–W_3O_{12}	1.71–1.71	O_4O_5	1.51
O_4O_6–O_5O_7	1.51–1.51	W_2O_5	1.95
O_8O_{10}	1.52	O_7O_9–O_8O_{10}	1.52–1.54
W_2O_{13}–W_3O_{14}	2.06–2.00	W_2O_{13}–W_3O_{14}	2.07–2.03
PO_{13}–PO_{14}	1.50–1.51	PO_{13}–PO_{14}	1.50–1.52
PO_{15}–PO_{16}	1.57–1.57	PO_{15}–PO_{16}	1.57–1.57
$O_4W_2O_5$–$O_5W_3O_4$	69.6–66.1	$O_4W_2O_5$	44.4
$O_4W_2O_6$–$O_5W_3O_7$	44.7–44.2	$O_7W_2O_9$–$O_8W_3O_{10}$	46.2–47.0
$O_8W_2O_{10}$	46.2	$O_4W_2O_6$–$O_4W_3O_6$	69.0–68.7
$O_{11}W_2O_5$	166.6	$O_{11}W_2O_6$–$O_{12}W_3O_4$	165.5–170.6
$O_{12}W_3O_4$–$O_9W_3O_4$	170.8–84.2		

[a] See Fig. 4 for the atomic numbering scheme. Bond distances, Å; valence angles, degrees.

TABLE 3

E_{LYP} Energy Values for Complexes A, B, and C and for the Ethylene, Ethylene Oxide, Hydrogen Peroxide, and Water Molecules

Complexes	E_{LYP}[a]
A	−1522.9267165
$\mathbf{B_1}$	−1448.2604150
$\mathbf{B_2}$	−1448.2663713
$\mathbf{C_1}$	−1373.5845352
$\mathbf{C_2}$	−1373.5867060
$\mathbf{C_3}$	−1373.5696530
Molecules	**E_{LYP}[a]**
Ethylene	−78.0960020
Ethylene oxide	−152.7979990
H_2O_2	−150.5762736
H_2O	−75.9225900

[a] Energy values in atomic units (1au = 27.21 eV = 2622.9 kJ · mol^{-1}) obtained from HF calculations and corrected by electron correlation contributions evaluated with the Lee, Yang, and Parr density functional (see text).

TABLE 4

Theoretically Evaluated Geometrical Parameters for Complexes $[H_2PO_4(W_2O_8)]^-$ (C)

Geometrical parameter[a]	C_1 computed value	Geometrical parameter[a]	C_2 computed value	Geometrical parameter[a]	C_3 computed value
W_2O_4–W_3O_5	2.06–2.07	W_2O_4–W_3O_6	2.09–1.79	W_3O_5–W_2O_4	1.78–1.79
W_2O_5–W_3O_4	2.27–2.31	W_3O_4–W_2O_6	2.32–2.21	W_2O_5–W_3O_4	2.33–2.34
W_2O_6–W_3O_7	1.93–1.95	W_2O_5	1.94	W_2O_8–W_2O_6	1.90–1.97
W_2O_9–W_2O_{10}	1.72–1.71	W_3O_9–W_3O_7	1.89–1.97	W_3O_9–W_3O_7	1.90–1.98
W_3O_{11}–W_3O_8	1.71–1.72	W_2O_{10}–W_2O_8	1.71–1.72	W_2O_{10}–W_3O_{11}	1.71–1.70
O_4O_6–O_5O_7	1.51–1.51	W_3O_{11}	1.70	O_6O_8–O_7O_9	1.53–1.54
W_2O_{12}–W_3O_{13}	2.07–2.03	O_4O_5–O_7O_9	1.51–1.54	W_2O_{12}–W_3O_{13}	2.03–2.05
PO_{12}–PO_{13}	1.51–1.51	W_2O_{12}–W_3O_{13}	2.08–2.03	PO_{12}–PO_{13}	1.51–1.51
PO_{14}–PO_{15}	1.57–1.57	PO_{12}–PO_{13}	1.51–1.52	PO_{14}–PO_{15}	1.57–1.57
$O_5W_3O_4$–$O_4W_2O_5$	68.7–69.7	PO_{14}–PO_{15}	1.58–1.57	$O_4W_3O_5$–$O_4W_2O_5$	68.5–68.6
$O_5W_3O_7$–$O_4W_2O_6$	44.0–44.3	$W_2O_4W_3$–$W_3O_6W_2$	101.3–117.0	$W_2O_4W_3$–$W_3O_5W_2$	108.9–109.4
$O_9W_2O_5$–$O_{10}W_2O_5$	87.4–164.7	$O_4W_2O_6$–$O_6W_3O_4$	69.0–71.5	$O_7W_3O_9$–$O_6W_2O_8$	46.6–46.7
$O_8W_3O_4$–$O_{11}W_3O_4$	85.4–169.0	$O_4W_2O_5$	43.9	$O_{10}W_2O_5$–$O_{11}W_3O_4$	172.6–168.8
		$O_7W_3O_9$	47.0		
		$O_{11}W_3O_4$	170.6		
		$O_8W_2O_6$–$O_{10}W_2O_6$	88.7–167.0		

[a] See Fig. 5 for the atomic numbering scheme. Bond distances, Å; valence angles, degrees.

bridging oxygen atoms in **C_3**. The computed E_{LYP} energies (Table 3) show that isomer **C_2** is the most favourable form, followed by **C_1** and **C_3**, lying 5.7 and 44.7 kJ · mol^{-1} higher in energy, respectively.

As shown in Table 4, the differences in the coordination environments of the three isomers **C_1**, **C_2**, and **C_3** have only a quite-limited effect on the computed values for bond distances, which, for homologous bond types, are all equal within the range ±0.03 Å.

The two isomers **C_2** and **C_1** that are very close in energy, may be expected to interconvert by a concerted breaking of the O(7)–O(9) bond and formation of an O(6)–O(9) bond or vice versa (the numbering refers to isomer **C_2**; see Fig. 5). This view is in agreement with the experimental observation of exchange between oxo and peroxo assigns in vanadium (V) and molybdenum (VI) complexes (20a). In the latter species, however, this exchange seems to be excluded on the basis of 170 NMR studies (20a). The conversion of **C_2** into **C_3**, on the contrary, would require the breaking of the O(4)–O(5) bond of **C_2** and formation of an O(5)–O(8) bond. This, however, produces an energetically unfavourable coordination, in which two bridging oxygen atoms are simultaneously present, without any significant bonding interaction between them. In fact, the distance O(4)–O(5) in **C_3** (2.36 Å) is much longer than that computed for O–O bonds of nonbridging and bridging peroxo group.

It is important to stress again that all the above results were obtained by a constraint-free geometry optimisation. This indicates that the presence of bridging oxygen atoms and/or bridging O_2 groups is intrinsically required by the energetics of the various complexes. Alternatively, one can also conclude that the occurrence of bridging O atoms is required to maximise the coordination number of each W atom, which is never smaller than six. Forms with pentacoordinated W atoms are expected to lie much higher in energy and, therefore, to be irrelevant as intermediate species.

*3.4. The Energetics of the Epoxidation Reaction with Peroxo Complexes **A** and **$B_{1,2}$***

In principle, the peroxo complexes **A**, **$B_{1,2}$**, and **C_{1-3}** described in Sections 1 and 2 can all be involved, as either reactants, or intermediates, or coproducts, in the oxygen transfer to alkene, according to the general equations [1] and [2].

The feasibility of each of the above epoxidation reactions (and, thence, also the reactivity of the peroxo complex involved) was verified on the basis of the reaction energy, which was evaluated using the E_{LYP} values for the respective reactants and products (Table 3). The following definition of the reaction energy ΔE is introduced: $\Delta E = [E_{LYP}(\text{product}) - E_{LYP}(\text{reactant})]$. Negative ΔE values indicate exothermic processes.

The evaluated energy for each reaction of Eq. [1] or [2] is reported in Table 5, together with the type of peroxo group involved in the oxygen transfer to ethylene.

Inspection of the data of Table 5 first of all reveals that the epoxidation reactions represented by Eqs. [1] and [2], to a different extent, have all an exoergic character and, thence, are all allowed from the energetic point of view. Moreover, it shows that oxygen transfer from complex **A** to ethylene (reactions [1.1] and [1.2]) is energetically favoured as compared to oxygen transfer from the intermediate species **B_1**

TABLE 5

Reaction Energies ΔE for the Epoxidation Reactions of General Equations [1] or [2]

Reaction	ΔE[a]	Reaction type[b]	Type of peroxo group involved
$\mathbf{A} + \mathbf{C_2}H_4 \rightarrow \mathbf{C_2}H_4O + \mathbf{B_1}$	−93.6	[1.1]	Nonbridging
$\mathbf{A} + \mathbf{C_2}H_4 \rightarrow \mathbf{C_2}H_4O + \mathbf{B_2}$	−109.2	[1.2]	Bridging
$\mathbf{B_1} + \mathbf{C_2}H_4 \rightarrow \mathbf{C_2}H_4O + \mathbf{C_1}$	−68.5	[2.1]	Nonbridging
$\mathbf{B_1} + \mathbf{C_2}H_4 \rightarrow \mathbf{C_2}H_4O + \mathbf{C_2}$	−74.2	[2.2]	Bridging
$\mathbf{B_2} + \mathbf{C_2}H_4 \rightarrow \mathbf{C_2}H_4O + \mathbf{C_2}$	−58.8	[2.3]	Nonbridging
$\mathbf{B_2} + \mathbf{C_2}H_4 \rightarrow \mathbf{C_2}H_4O + \mathbf{C_3}$	−13.8	[2.4]	Bridging

[a] All the reported values are expressed in $kJ \cdot mol^{-1}$.
[b] Reaction numbering is taken from Eqs. [1] and [2] of the text.

and $\mathbf{B_2}$ to the same substrate (reactions [2.1]–[2.4]), the energy gain being up to more than 30% in the former case and even more in the latter.

From the comparison of the energies of reactions [1.1] and [1.2] it also emerges that the involvement of a bridging O_2 group in the oxidative process is favoured from the thermodynamic point of view as compared to that of a normal coordinated peroxo group. A similar trend, with the O_t oxygen atoms being again slightly more favoured energetically than those of normal O_2 group, is computed also for the oxygen transfer from $\mathbf{B_1}$ to ethylene (reactions [2.1] and [2.2]), while an opposite trend is computed for the analogous oxygen transfer from $\mathbf{B_2}$ (reactions [2.3] and [2.4]), where the exothermicity of the reaction involving the O_t atoms is the lowest among all the considered cases.

The trend in computed energies for reactions involving a different type of oxygen atoms, O_{t2}, O_{t1}, O_d, can be qualitatively correlated with the total bond orders derived from the Mulliken analysis. The bond order (BO) for of a given oxygen atom is here defined as the sum of contributions (atom–atom overlap population) due to all other atoms and it can be considered as proportional to the strength by which the atom itself is bound to the complex and, therefore, representative of the difficulty by which the oxygen atom is transferred to the substrate. BO values equal to 0.280, 0.236, 0.260, and 0.255 have been computed for O_{t2}, O_{t1} and the two nearly equivalent O_d oxygen atoms, respectively. For comparison, the BO value for the oxo atom O_s has been computed as equal to 0.400. When the BO value of a given oxygen atom is assumed to be a measure of its tendency to react, then the order $O_{t1} > O_d > O_{t2} > O_s$ can be established, which is in a qualitative agreement with that based on the computed reaction energies. In addition, the BO values allow pointing out that within the bridging peroxo group the strong interaction with both metal centres of the triply shared oxygen atom is accompanied by a weakening of the O–O bond.

*3.5. The Charge Distribution in Complexes **A** and $\mathbf{B_{1,2}}$ vs the Energetics of the Epoxidation Reaction*

It may be appropriate at this point to examine the net atomic charges computed for the various atoms of complexes **A**, $\mathbf{B_1}$, and $\mathbf{B_2}$ (Table 6).

As mentioned at the beginning of this paper, the presence in the $\{PO_4[W(O)(O_2)_2]_4\}^{3-}$ anion of dissymmetric bridging peroxo groups, in which a pronounced polarisation of the O–O bond would lead to one oxygen atom being more electrophilic than the other, has been assumed (4, 8) as a possible explanation of the high epoxidizing activity of this species. Such a hypothesis is now tested on the model complex **A** against the computed values of the Mulliken electron populations.

In complex **A**, the oxygen atoms belonging to the phosphate group are the most negatively charged (−0.73, average value), followed by the terminal O_s atoms (−0.51). Interestingly, the normal and bridging O_2 groups carry a quite similar total charge (−0.86 and −0.91, respectively). However, in the nonbridging peroxo group, the charge is distributed over the two oxygens in a very balanced way (−0.44 over one oxygen and −0.42 over the other), while in the bridging peroxo group it appears to be partially polarised, being accumulated more on the triply shared oxygen O_{t2} (−0.53) than on the oxygen adjacent, O_{t1} (−0.38), which is thus the least negatively charged atom among all peroxidic oxygens of complex **A**. O_{t1} would be therefore expected to be the best candidate to interact with an electron

TABLE 6

Mulliken Net Atomic Charges for Tungsten(VI) Peroxo Complexes A, B, and C

	Complex					
	A	$\mathbf{B_1}$	$\mathbf{B_2}$	$\mathbf{C_1}$	$\mathbf{C_2}$	$\mathbf{C_3}$
Atom	Charge					
P	1.728	1.725	1.700	1.711	1.698	1.707
W_2	1.943	1.949	1.920	1.738	1.695	1.788
W_3	1.943	1.733	1.847	1.733	1.845	1.778
O_4	−0.529	−0.529	−0.520	−0.547	−0.527	−0.711
O_5	−0.529	−0.541	−0.397	−0.547	−0.420	−0.699
O_6	−0.376	−0.386	−0.738	−0.404	−0.742	−0.432
O_7	−0.376	−0.405	−0.443	−0.408	−0.432	−0.438
O_8	−0.444	−0.444	−0.432	−0.563	−0.564	−0.461
O_9	−0.444	−0.561	−0.433	−0.563	−0.454	−0.466
O_{10}	−0.419	−0.430	−0.447	−0.561	−0.560	−0.543
O_{11}	−0.419	−0.528	−0.525	−0.559	−0.542	−0.540
O_{12}	−0.514	−0.556	−0.536	−0.733	−0.729	−0.741
O_{13}	−0.514	−0.728	−0.725	−0.747	−0.751	−0.734
O_{14}	−0.736	−0.753	−0.749	−0.706	−0.702	−0.698
O_{15}	−0.736	−0.714	−0.701	−0.712	−0.698	−0.693
O_{16}	−0.715	−0.714	−0.698			
O_{17}	−0.715					
H	0.426	0.438	0.448	0.434	0.442	0.441

rich site, like the π system of an unsaturated substrate, according to the "electrophilic" mechanism proposed for the oxygen transfer from early-transition-metal peroxo complexes to olefins (1b, 2, 21).

The prediction in complex **A** of a higher reactivity towards alkenes for the O_{t1} oxygen, compared to the O_d oxygens, based on the charge density (taken as rough measure of the electrophilic character) turns out to be in accord with the thermodynamic data. In fact, as already discussed above (cf. Table 5), oxygen transfer from the bridging peroxo group of **A**, which just contains O_{t1} (Eq. [1.2]) also leads to a species more stable than that formed subsequent to oxygen transfer from the nonbridging peroxo group containing the O_d oxygens (Eq. [1.1]) ($\Delta E = -109.2$ vs -93.6 kJ · mol^{-1}).

Now, the question may be raised whether the observed correlation between a lower net charge over one of the oxygen centres of a peroxo group and a higher reaction energy of the group itself when involved in the oxygen transfer to alkene holds also for species other than **A**. The answer is not univocal, as results from the examination of the complexes of type **B**.

For isomer $\mathbf{B_1}$, the peroxidic oxygens of type O_d, O_{t1}, and O_{t2} carry net charges equal to -0.44, -0.39, and -0.53, respectively (Table 6). As shown before (cf. Table 5), the oxygen transfer from a bridging, rather than a normal peroxo group of $\mathbf{B_1}$ (Eqs. [2.2] and [2.1], respectively) corresponds to a somewhat higher energy gain ($\Delta E = -74.2$ vs -68.5 kJ · mol^{-1}). Again, the reaction involving the peroxo group that contains the least negatively charged oxygen atom, O_{t1}, is also the one favoured energetically.

The trend is just the opposite for isomer $\mathbf{B_2}$; here the peroxidic oxygen atom O_{t1}, expected to be "more electrophilic" than the O_d oxygens based on the charge density (-0.40 vs -0.44 (average value); Table 6), is not associated with a higher exothermicity. Indeed, from Table 5 it turns out that the epoxidation reaction involving the nonbridging peroxo group of $\mathbf{B_2}$ (Eq. [2.3]) is characterised by an energy release definitely larger than that which accompanies the reaction involving the bridging peroxo group (Eq. [2.4]) ($\Delta E = -58.6$ vs -13.8 kJ · mol^{-1}).

The situation can be summarised as follows: The trend of the atomic net charges on the peroxidic oxygen atoms in complexes **A**, $\mathbf{B_1}$, and $\mathbf{B_2}$ is very similar. Accordingly, the O_{t1} oxygens adjacent to the triply shared O_{t2} oxygens would be expected in all cases to exhibit an electrophilic character stronger than the O_d ones, based on their lower charge density. However, the "more electrophilic" site O_{t1} and the "less electrophilic" sites O_d are clearly differentiated also in terms of reaction energy only in the case of complex **A** and, less markedly, of complex $\mathbf{B_1}$, while their energetic difference is even reversed in complex $\mathbf{B_2}$. In this last case, therefore, no prediction of the relative reactivity of the O_{t1} and O_d sites is possible.

3.6. The Thermodynamic Cycle

The epoxidation reactions of general Eqs. [1] and [2] discussed above may be regarded as steps of the following thermodynamic cycles (i) and (ii), where hydrogen peroxide is the terminal oxidant:

(i) $A + C_2H_4 \rightarrow C_2H_4O + B_x \quad (x = 1, 2)$
$B_x + H_2O_2 \rightarrow H_2O + A$

(ii) $B_x + C_2H_4 \rightarrow C_2H_4O + C_y \quad (x = 1, 2;\ y = 1\text{–}3)$
$C_y + H_2O_2 \rightarrow H_2O + B_x.$

Clearly, the sum of the reactions in (i) or (ii) corresponds to the gas phase epoxidation reaction with hydrogen peroxide as the only oxidant (Eq. [3]):

$$H_2O_2 + C_2H_4 \rightarrow C_2H_4O + H_2O. \qquad [3]$$

The reaction energy for [3], computed with the same theoretical approach used to evaluate the energies ΔE for reactions [1] and [2] involving complexes **A**–**C** (Table 3), was equal to -126.7 kJ · mol^{-1}. On the basis of experimental estimates, the heat of reaction for the epoxidation of a double bond with hydrogen peroxide has been reported to be about -250 kJ · mol^{-1} (22). In our opinion, such a value is probably overestimated. In order to prove such a point, we recomputed the ΔE value for reaction [3] using a much larger basis set (including polarisation functions, STO-631* (10)) and a fully iterative density functional approach (12, 23) which takes into account correlation effects also for geometry optimisation. The ΔE value thus obtained was -182 kJ · mol^{-1}, still considerably smaller than the estimate of Ref. (22).

Using the E_{LYP} values of Table 3, the energies for the reoxygenation processes of species $\mathbf{B_x}$ in (i) and $\mathbf{C_y}$ in (ii) with hydrogen peroxide can be easily computed. They are reported in Table 7.

The data of Table 7 show that, analogously to reactions [1] and [2], also the above "recharge" processes are reactions that are not forbidden from the energetic point of

TABLE 7

Reaction Energies ΔE for the Reoxygenation of Complexes B and C with Hydrogen Peroxide

Reaction	ΔE^a
$\mathbf{B_1} + H_2O_2 \rightarrow \mathbf{A} + H_2O$	-33.1
$\mathbf{B_2} + H_2O_2 \rightarrow \mathbf{A} + H_2O$	-17.5
$\mathbf{C_1} + H_2O_2 \rightarrow \mathbf{B_1} + H_2O$	-58.2
$\mathbf{C_2} + H_2O_2 \rightarrow \mathbf{B_1} + H_2O$	-52.5
$\mathbf{C_2} + H_2O_2 \rightarrow \mathbf{B_2} + H_2O$	-68.1
$\mathbf{C_3} + H_2O_2 \rightarrow \mathbf{B_2} + H_2O$	-112.8

[a] All the reported values are expressed in kJ · mol^{-1}.

view. Obviously, the smaller exothermicity of the epoxidation reactions involving complexes of type **B** implies a higher exothermicity for the "recharge" processes from the related complexes of type **C**. It should also be noted that reoxygenation reactions from species $\mathbf{B_2}$, $\mathbf{C_2}$, or $\mathbf{C_3}$ (not shown here) envisaged to lead to products other than the precursors are all largely unfavourable energetically. It follows that only the reoxygenation reactions which give back (directly or in a two-step sequence) the starting complex **A** are possible between hydrogen peroxide and species of type **B** or **C**. This allows us to conclude that the global processes indicated in (i) and (ii) can always occur, at least from a thermodynamic point of view.

4. CONCLUSIONS

On the basis of our theoretical *ab initio* study concerning the structure/reactivity (towards alkenes) relationships of model anionic tungsten(VI) peroxo complexes derived from the $\{PO_4[W(O)(O_2)_2]_4\}^{3-}$ complex, the following conclusions can be drawn.

All the considered epoxidation reactions between complex **A** (the basic species in this work) or the "partially reduced" complexes of type **B** and ethylene (the alkene chosen for this study) are found to be exothermic, with the oxygen transfer from **A** being more favourable energetically than that from **B**. Also the "recharge" reactions of the resulting "reduced" complexes with hydrogen peroxide, leading to the precursors and, in any case, to the starting complex **A**, are exothermic processes. This ensures the possibility of existence of the global processes (i) and (ii), at least from the thermodynamic point of view.

On the basis of the computed reaction energies and of the electrophilic character of each peroxidic oxygen roughly estimated from its net atomic charge, the bridging peroxo group is suggested to be primarily involved in the olefin epoxidation by complex **A**, with the O_{t1} oxygen being presumably transferred to an alkene.

These data support the advanced assumption (4, 8) that the dissymmetry of the peroxo ligand, with one oxygen being made more electrophilic than the other by the O–O bond polarisation, favours oxygen transfer to the nucleophilic substrate. However, no generalisation of this view can be drawn from the study, as the reaction energy of a peroxo group does not correlate regularly with the electrophilic character of its sites, at least when the electrophilic character is defined in terms of the atomic net charge only. Indeed, such a correlation, while seeming to be qualitatively valid for complex **A** and also for complex $\mathbf{B_1}$, breaks down for complex $\mathbf{B_2}$. Analogously, also the reactivity order of the different oxygen atoms cannot be derived from simple considerations based on bond orders.

This might mean that for $\mathbf{B_2}$ the oxygen transfer to an alkene is thermodynamically controlled. Alternatively, the discrepancy might be ascribed to the fact that the electrophilic character of a site cannot necessarily be determined from its charge density, or it might also be a consequence of the limitations of this study, which is clearly unable, in the present form, to evaluate the kinetic aspects of the examined reactions.

For this last reason, of course, the study cannot give information about the relative efficiency of the global processes (i) and (ii) and, thence, about the real nature of the catalytic cycle, although the data obtained would suggest cycle (i) to be mainly operative under turnover conditions, as the reoxygenation of metal oxo species with hydrogen peroxide is known to be far faster than the epoxidation reaction (2, 18, 24). This point requires much more elaborate and detailed investigation of the electronic and energy characteristics of the transition states of the individual reaction paths. All these aspects are planned to be present in a future study.

It is worth pointing out that, on the basis of kinetic and spectroscopic evidence, a transformation analogous to that indicated in (i), which may schematically be represented as $\mathbf{A} \rightleftarrows \mathbf{B}$, has been recently reported (19) to be the dominant process in the olefin epoxidation with hydrogen peroxide catalysed by the $\{PO_4[W(O)(O_2)_2]_4\}^{3-}$ species under turnover conditions.

ACKNOWLEDGMENTS

This work was supported by Italian CNR (Rome) and by EniChem Ricerche.

REFERENCES

1. For reviews, see: (a) Pralus, M., Lecoq, J. C., and Schirmann, J. P., "Fundamental Research in Homogeneous Catalysis" (M. Tutsui, Ed.), Vol. 3, p. 327. Plenum, New York, 1979; (b) Sheldon, R. A., and Kochi, J. K., "Metal-Catalyzed Oxidations of Organic Compounds," Academic Press, New York, 1981; (c) G. Strukul (Ed.), "Catalytic Oxidations with Hydrogen Peroxide as Oxidant," Vol. 9, Kluwer Academic, Amsterdam, 1992.
2. Di Furia, F., and Modena, G., *Pure Appl. Chem*. **54**, 1853 (1982).
3. Venturello, C., Alneri, E., and Ricci, M., *J. Org. Chem*. **48**, 3831 (1983).
4. Venturello, C., D'Aloisio, R., Bart, J. C. J., and Ricci, M., *J. Mol. Catal*. **32**, 107 (1985).
5. Venturello, C., and D'Aloisio, R., *J. Org. Chem*. **53**, 1553 (1988).
6. Jian, X., and Hay, H., *J. Pol. Sci.: Part C: Pol. Lett*. **28**, 285 (1991); **29**, 547 (1991).
7. (a) Amato, G., Arcoria, A., Ballistreri, F. P., Tomaselli, G. A., Bortolini, O., Conte, V., Di Furia, F., and Modena, G., *J. Mol. Catal*. **37**, 165 (1986); (b) Campestrini, S., Conte, V., Di Furia, F., and Modena, G., *J. Org. Chem*. **53**, 5721 (1988); (c) Arcoria, A., Ballistreri, F. P., Spina, E., Tomaselli, G. A., and Toscano, R. M., *Gazz. Chim. Ital*. **120**, 309 (1990).
8. Csányi, L. J., and Jáky, K., *J. Catal*. **127**, 42 (1991).
9. Hay, P. J., and Wadt, W. R., *J. Chem. Phys*. **82**, 299 (1985).
10. Hehre, W. T., Random, L., Schleyer, P. v. R., and Pople, J., "Ab initio Molecular Orbital Theory," Wiley-Interscience, New York, 1986.

11. Guest, M. F., Kendrick, J., van Lenthe, J. H., Schoeffel, K., and Sherwood, P., Gamess-UK Program, Version 5.
12. Lee, C., Yang, W., and Parr, G., *Phys. Rev.* **82**, 299 (1985).
13. Fantucci, P., Polezzo, S., Bonacic-Koutecky, V., and Koutecky, J., *J. Chem. Phys.* **92**, 6645 (1990).
14. Murray, C. W., Laming, G. J., Handy, N. C., and Amos, R. D., *Chem. Phys. Lett.* **199**, 551 (1992).
15. (a) Mulliken, R., *J. Chem. Phys.* **23**, 1833 (1955); **23**, 2343 (1955); (b) Mc Weeny, R., *J. Chem. Phys.* **19**, 1614 (1951); **20**, 920 (1952).
16. (a) Cioslowski, J., Hay, P. J., and Ritchie, P., *J. Phys. Chem.* **94**, 148 (1990); (b) Levine, N., "Quantum Chemistry," Prentice–Hall, Englewood Cliffs, NJ, 1991.
17. Salles, L., Aubry, C., Thouvenot, R., Robert, F., Dorémieux-Morin, C., Chottard, G., Ledon, H., Jeannin, Y., and Brégeault, J.-M., *Inorg. Chem.* **33**, 871 (1994).
18. Jacobson, S. E., Muccigrosso, D. A., and Mares, F., *J. Org. Chem.* **44**, 921 (1979).
19. Duncan, D. C., Chambers, R. C., Hecht, E., and Hill, C. L., *J. Am. Chem. Soc.* **117**, 681 (1995) and references therein.
20a. Bortolini, O., Di Furia, F., and Modena, G., *J. Am. Chem. Soc.* **103**, 3924 (1981).
20b. Postel, M., Brevard, C., Arzoumanian, H., and Riess, J. G., *J. Am. Chem. Soc.* **105**, 4922 (1983).
21. Sharpless, K. B., Townsend, J. M., and Williams, D. R., *J. Am. Chem. Soc.* **94**, 295 (1972).
22. Quaglino, M., Bottazzini, N., Querci, C., Ricci, M., and Cavalli, S., *J. Am. Oil Chem. Soc.* **69**, 1248 (1992).
23. Becke, A. D., *Phys. Rev.* **A38**, 3098 (1988).
24. Bortolini, O., Campestrini, S., Di Furia, F., and Modena, G., *J. Org. Chem.* **52**, 5093 (1987) and references therein.